

Antibacterial Broad-Spectrum Dendritic/Gellan Gum Hybrid Hydrogels with Rapid Shape-Forming and Self-Healing for Wound Healing Application

Giuseppina Biscari, Yanmiao Fan, Faridah Namata, Calogero Fiorica, Michael Malkoch,*
Fabio Salvatore Palumbo, and Giovanna Pitarresi

Treating wound infections is a difficult task ever since pathogenic bacteria started to develop resistance to common antibiotics. The present study develops hybrid hydrogels based on the formation of a polyelectrolyte complex between the anionic charges of dopamine-functionalized Gellan Gum (GG-DA) and the cationic moieties of the TMP-G2-alanine dendrimer. The hydrogels thus obtained can be doubly crosslinked with CaCl_2 , obtaining solid hydrogels. Or, by oxidizing dopamine to GG-DA, possibly causing further interactions such as Schiff Base and Michael addition to take place, hydrogels called injectables can be obtained. The latter have shear-thinning and self-healing properties (efficiency up to 100%). Human dermal fibroblasts (HDF), human epidermal keratinocytes (HaCaT), and mouse monocyte cells (RAW 264.7), after incubation with hydrogels, in most cases show cell viability up to 100%. Hydrogels exhibit adhesive behavior on various substrates, including porcine skin. At the same time, the dendrimer serves to crosslink the hydrogels and endows them with excellent broad-spectrum microbial eradication activity within four hours, evaluated using *Staphylococcus aureus* 2569 and *Escherichia coli* 178. Using the same GG-DA/TMP-G2-alanine ratios hybrid hydrogels with tunable properties and potential for wound dressing applications can be produced.

One major mode of entry for microorganisms is the skin being the largest organ and the main defense barrier of the human body. In the event of a skin injury, infections and other uncontrolled pro-inflammatory factors can lead to chronic inflammatory reactions that can significantly delay wound healing and eventually lead to life-threatening sepsis phenomena.^[3,4] Typically, wound dressings are used to treat skin injuries to provide a physical barrier between the wound and the external environment.^[5] Advanced wound dressing solutions are developed to efficiently eradicate infections and thereof accelerate the recovery of the traumatized tissue. Hydrogels have been largely proposed in the past years as wound dressing thanks to their high-water content and high porosity, ability to act as reservoirs for loading and release of bioactive molecules as well as intrinsic properties of mimicking the extracellular matrix of native tissues.^[6,7] One intriguing strategy that the human body uses to fight invading microorganisms is the expression of endogenous cationic

antimicrobial peptides (AMPs) that possess a weak ability to bind to eukaryotic cells but can bind strongly to negatively charged bacterial walls causing a series of event that lead to cell death.^[8] With the rise of multidrug-resistant strains, research on the structure and mechanisms underlying these “endogenous defenders of the organism” has been of the greatest importance. This has resulted in the development of a new line of defense represented by macromolecules that mimic AMPs that can complement current antibiotics treatment.^[9–11] Cationic polyester dendrimers based on 2,2-bismethylol propionic acid (bis-MPA) are among the most fascinating cationic macromolecules that have AMP-mimicking properties.^[12,13] These dendrimers have highly branched 3D structures, inherent amphiphilic character, and rapid degradation profile. The multitude representation of active groups, allocated at the corona of the dendritic skeleton, are exposed to the surrounding environment resulting in a strong ability to bind the microbial cell wall.^[14–16] For example, bis-MPA dendrimers with β -alanine cationic functionality have great potential as antibacterial agents. In this case, a dendrimer of the second generation (G2) with 12 primary amino cationic groups

1. Introduction

The rapid emergence of antibiotic resistance in pathogenic bacteria is becoming an imminent global public health problem.^[1,2]

G. Biscari, C. Fiorica, F. S. Palumbo, G. Pitarresi
KTH Royal Institute of Technology
Teknikringen 56–58, Stockholm SE-100 44, Sweden
Y. Fan, F. Namata, M. Malkoch
University of Palermo
Via Archirafi 32, Palermo 90123, Italy
E-mail: malkoch@kth.se

 The ORCID identification number(s) for the author(s) of this article can be found under <https://doi.org/10.1002/mabi.202300224>

© 2023 The Authors. Macromolecular Bioscience published by Wiley-VCH GmbH. This is an open access article under the terms of the Creative Commons Attribution License, which permits use, distribution and reproduction in any medium, provided the original work is properly cited.

DOI: 10.1002/mabi.202300224

at the dendritic outer layer, TMP-G2-alanines, exhibited excellent AMP-mimicking properties with respect to bacterial killing efficacy and low cytotoxicity to human cells. At generation three or higher, these dendrimers showed cytotoxicity to human cells prior to degradation.^[12] To overcome such drawbacks, Fan and co-authors developed a series of hybrid hydrogels formed by physical interaction between cationic dendrimers, of generation two to four, and negatively charged cellulose nanofibrils (CNF) which increased their cytocompatibility against hDF and RAW 264.7 cells.^[17]

With the aim to develop a novel hydrogel platform with tunable viscoelastic properties to safely administer TMP-G2-alanines onto the wound bed, we produce a hybrid biomaterial composed of the multifunctional cationic polyester dendrimers and dopamine-functionalized low molecular weight Gellan-Gum. Gellan Gum (GG) is a linear exopolysaccharide with peculiar gelling properties that can depend on both the temperature and ionic strength of the surrounding medium.^[18,19] Also, the viscoelastic properties GG based dispersions can be easily modulated by varying the molecular weight of the starting macromolecule.^[20] Here, exploiting GG-polyanionic nature we demonstrated that is possible to obtain physical hydrogels simply upon mixing of the polysaccharide dispersion with the cationic dendrimer. Obtained physical hydrogels can be further cured with CaCl₂ solution to obtain double crosslinked solid-like hydrogels.

The presence of pendant catechol moieties on the polysaccharide backbone enables additive interactions with the dendrimer, such as Schiff Base and Michael addition, upon dopamine oxidation allowing to obtain fluid-like injectable hydrogel with self-healing and adhesive properties. On the whole, we demonstrated that the hydrogels' physicochemical and viscoelastic features are correlated to the precise hybridization of multifunctional cationic polyester dendrimers and dopamine-functionalized Gellan Gum and can be easily modulated by changing the external medium conditions thanks to the sensitiveness of GG and the presence of catechol moieties. This versatility along with the easiness of production represents an innovation compared to other hydrogels proposed so far as wound dressing as it makes it possible to modulate the dressing features depending on the characteristics of the wound to be treated.

Physicochemical and rheological characterizations were conducted for all the produced hydrogel to demonstrate the possibility to be effectively used as a wound dressing. Also, their cytocompatibility was assessed using different cell lines. Finally, the antibacterial properties were studied against two representative strains of Gram-positive and Gram-negative, *S. aureus* 2569 and *E. coli* 178 respectively.

2. Results and Discussion

2.1. Hybrid Hydrogels Production

The development of multifunctional wound dressings based on antibiotic-free hydrogels that efficiently promote the eradication of infection of damaged tissues is crucial to address existing healthcare challenges. An attractive materials solution that we hypothesized is the development of a novel platform of hydrogels that combines the unique properties of natural-

derived biomaterial and AMP-mimicking dendritic polymers. Consequently, we explored the hybridization of anionic GG-DA (of which the scheme of synthesis, FT-IR, and ¹H-NMR are reported in Figure S1, Supporting Information) together with the non-toxic and antibacterial cationic TMP-G2-alanine polyester dendrimer.^[12] Initial mixing of GG-DA and TMP-G2-alanine in aqueous conditions resulted in fragile and fragmented polyelectrolyte complex hydrogels. A strategy was therefore required that goes beyond simple ionic interaction and toward well-structured hybrid hydrogels with improved viscoelastic properties suited for biomedical applications.^[21] More specifically, the strategy was reinforced by implementing a dual-crosslinking approach by combining ionic self-assembly of the networks with a subsequent curing step in 0.1 M CaCl₂ at 4 °C for 1 h. The hydrogels, referred to as "solid" or "sol" hybrid hydrogels, with enhanced modulus were produced straightforwardly by simultaneous injection of the two-component solutions of GG-DA and TMP-G2-alanine into different molds, for example, a cylindrical mold, and then immersed in 0.1 M CaCl₂. 3D cylindrical hydrogels with dual crosslinks were obtained, first via physical ionic interactions between NH₃⁺ of the dendrimer and COO⁻ of the GG-DA polymer and then reinforced through ionotropic crosslinking of GG-DA with divalent Ca²⁺ ions that are interposed between the carboxyl groups represented on GG chains (Figure S2A, Supporting Information). Indeed, the proposed dual-crosslinked strategy improves the viscoelastic performance of the designed hydrogels. To detect the impact of crosslinking induced by Ca²⁺ ions on modulus, a rheological assessment of the hydrogels was conducted by comparing the crosslinking gelation process. For comparison, two representative hydrogel systems were produced and evaluated. In total, four different hydrogels were developed by mixing the precursors, i.e., two H1 (no CaCl₂) and H3 (no CaCl₂), and two more, H1 (CaCl₂) and H3 (CaCl₂) that were finally immersed in 0.1 M CaCl₂ for 1 h. To detect the effect of ion-induced crosslinking, the rheological profile of hydrogels based on GG-DA and TMP-G2-alanine was evaluated by comparing the crosslinking procedures, using only physical crosslinking or dual-crosslinking with 0.1 M CaCl₂. Frequency sweep analyses in Figure S3 (Supporting Information) revealed an order of magnitude higher G' and G'' values for the hydrogels with reinforced crosslinking with CaCl₂. These findings supported our initial hypothesis in which Ca²⁺ crosslinking with available pendant carboxylic groups further enhanced the modulus of the hybrid hydrogels. All solid hydrogels were then produced following the identified procedure. To further capitalize on the modularity of the proposed two-component hybrid hydrogels platform we further explored the feasibility to generate injectable hydrogels, referred to as injectable or inj hybrid hydrogels. Antibacterial hydrogels with injectable, remodeling, and self-healing properties can perfectly fill uneven wounds as on-demand topical hydrogel solutions for accelerated infectious wound healing.^[22] In this context, and in contrast to the Ca²⁺ crosslinking strategy, the oxidation of the pendant dopamine into dopa-quinone at elevated pH of 8.5 followed by mixing with TMP-G2-alanine dendrimer facilitated the development of injectable hydrogels. From the point of view of wound applicability, hydrogels would be readily oxidized in air and under oxidative conditions, which are also closely associated with bacterial colonization and lead the wound to approach an alkaline pH.^[23] The systems were found extrudable from a syringe

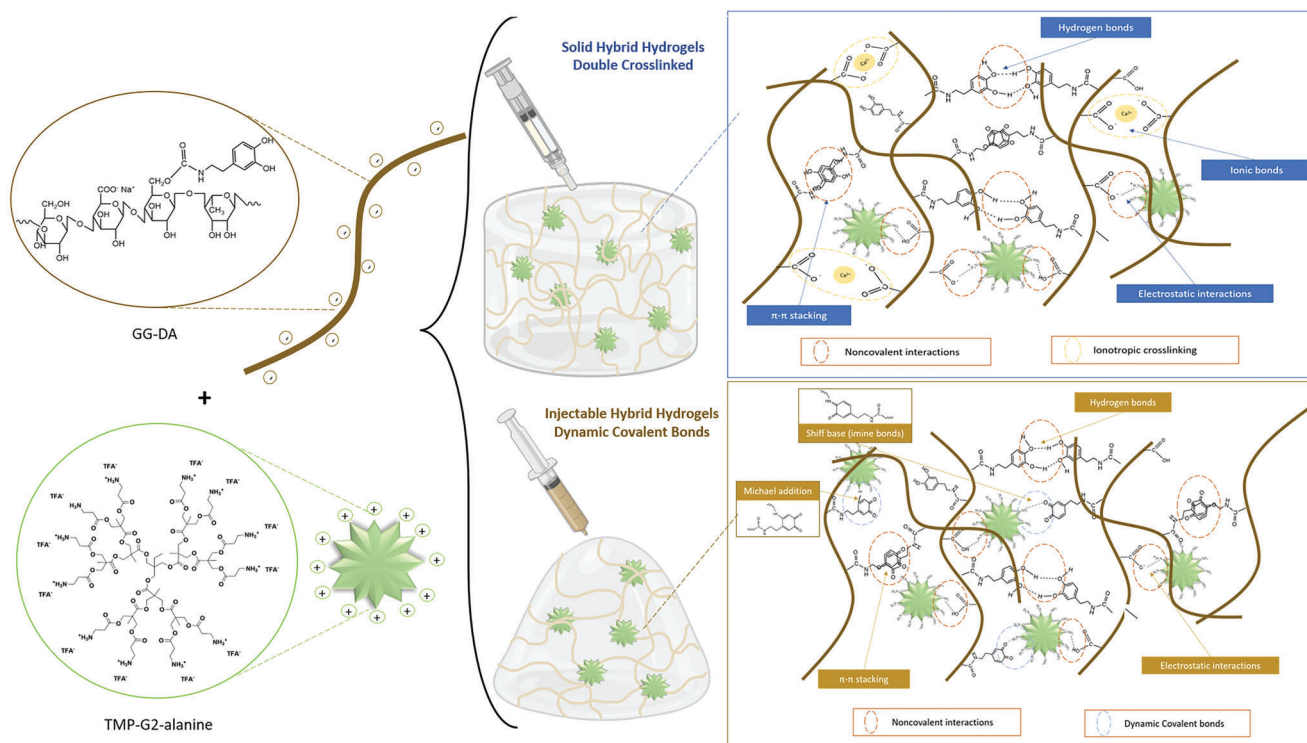


Figure 1. Schematic diagram describing the formation of solid hybrid hydrogels (above) and injectable hybrid hydrogels (below).

and post-injection of the mixture resulted in “soft” and homogeneous injectable hydrogels (Figure S2B, Supporting Information). These hydrogels are reinforced with a new set of crosslinking mechanisms, such as the imine bond by Schiff Base and Michael addition, which together with the non-covalent physical bonds present in the already formed polyelectrolyte complex, give these injectability and self-healing properties.^[24] The formation of both solid and injectable hybrid hydrogel types is shown in the scheme in **Figure 1**.

2.2. Characterization

FTIR analysis was used to determine the presence of dendrimers within both hybrid hydrogels. In **Figure 2A**, representative spectra of two hybrid hydrogels, H1_{sol} and H1_{inj} (3%w/v GG-DA and 100%w/w TMP-G2-alanine with respect to GG-DA) are shown in comparison with the spectra of TMP-G2-alanine, GG-DA, and the H1k (3%w/v GG-DA alone in 0.1 M CaCl₂), produced from GG-DA alone. The peaks at 1733 and 1667 cm⁻¹ are characteristic of the C=O due to the carbonyl ester and of the deformation vibration peak of -NH₂ in the dendrimer. Both peaks were observed in the spectra of the solid and injectable hybrid hydrogels H1 as well as for the pure dendrimer sample. Swelling of hybrid hydrogels was evaluated for up to 48 h in which the injectable hydrogels showed higher swelling behavior than the solid hydrogels, **Figure 2C,D**. Additionally, the injectable hydrogels exhibited a two-fold swifter swelling capacity reaching a plateau after 4 h compared to the solid hydrogels that required 8 h. The values are shown in **Table 1**. The swelling capacity of the control

hydrogels and solid hybrid hydrogels was studied for up to 48 h. However, the structural integrity of the injectable hydrogels was compromised after 24 h, and swelling data were collected within that time frame. The control hydrogels, H1k and H2k, elucidated lower swelling capacity than hybrid hydrogels. This could be reasoned to the formation of more compact polymer networks based on ionic crosslinks between the available carboxylate groups of GG-DA and the divalent Ca²⁺. For the hybrid systems, hydrogels with the lowest percentages of both GG-DA and TMP-G2-alanine, called H2, noted the highest swelling percentage (after 24 h, ≈1267% for the solid and ≈1768% for the injectable). This can be compared to the compared to H3 reaching ≈1145% for the solid and ≈1438% for the injectable hydrogels after 24 h. With over tenfold water swelling capacity these hydrogels have the potential to scavenge skin wound exudate that contains nutrients necessary for bacterial growth and lead to skin maceration.^[25] **Figure 2B** shows the SEM image of the section of lyophilized H1_{sol}. The image of the dehydrated hydrogel shows a spongy-like porous network. This typical structure could promote swelling, interactions with biological fluids, and gaseous exchanges. In **Figure S4** (Supporting Information) there are also the SEM analyses of the hydrogels H1_{inj}, and H1k, which have similar structures to the previous hydrogel. The degradation properties of wound dressing materials are important as it is essential to meet the skin's requirements in remodeling and inducing morphogenesis to form new tissues.^[26] A degradation study was carried out both in terms of recovered weight% compared to the original weight and also in terms of viscoelastic properties over time. Amplitude and frequency sweep rheological degradation study was performed in phosphate-buffered saline (PBS pH 7.4) at

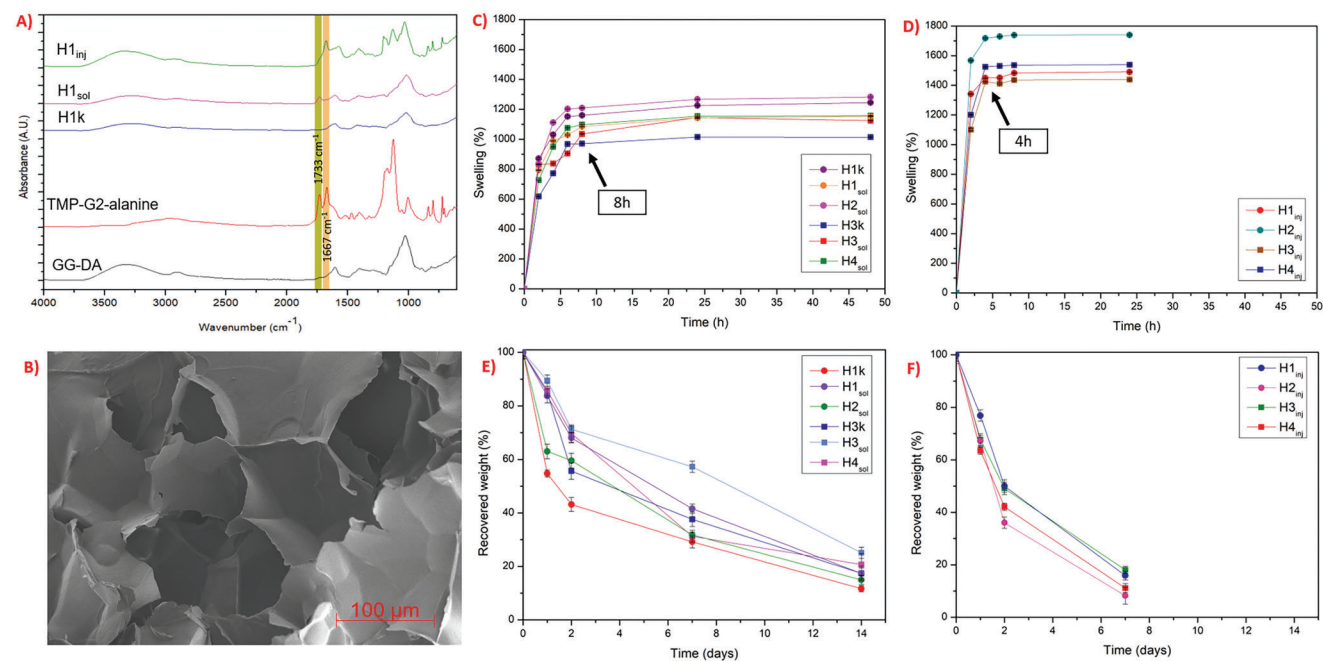


Figure 2. Characterization of the hybrid hydrogels. A) FT-IR of representative solid, injectable, and control hydrogels, TMP-G2-alanine, and GG-DA. B) SEM image of the H1_{sol} as a representative sample. Swelling behavior of solid, C) control, and D) injectable hydrogels. Hydrolytic degradation of solid, E) control, and F) injectable hydrogels.

37 °C. The injectable hydrogels degraded faster, reaching less than 50% of their original weight within 2 days (Figure 2F), than the solid hydrogels that required 7 days for 50% loss of their original weight (Figure 2E). In general, all solid and control hydrogels could be recovered for up to 14 days, while injectable hydrogels were completely degraded. The solid hydrogel with the highest polymer and dendrimer content, H3_{sol}, showed greater degradation resistance than all hybrid hydrogels with ≈60% weight recovered after 7 days (Table 1). From the amplitude sweep rheograms, after each time of incubation, it can be seen that the Storage modulus (G') and the Loss modulus (G'') decrease, confirming that the networks undergo degradation as shown in Figures S5

and S6 (Supporting Information). Furthermore, from frequency sweep rheograms, the decrease in the elastic behavior is probably attributable not only to the degradation and release of the dendrimer but also, in the solid hydrogels, to the possible depletion of calcium from the 3D structure (Figures S7 and S8, Supporting Information). Overall, the collected data indicates that the hybrid hydrogels possess adjustable properties and by varying the concentrations of the two biomaterials different degradation rates are obtained. Hydrogels produced using these two materials could potentially be administered to treat infection in the first few days after injury to allow the healing process to resume.

Table 1. Summary data of swelling, degradation, and rheological of hydrogels.

Sample	Swelling plateau [%]	Recovered weight [%] after 7 days	Amplitude sweep			Frequency sweep		Flow sweep	Recovery time			
			G' [kPa]	G'' [kPa]	Cross-point strain%	G' [kPa]	G'' [kPa]		G' [kPa] (1% strain)	G'' [kPa] (1% strain)	G' [kPa] (500% strain)	G'' [kPa] (500% strain)
H1k	1160	30	9.9	3.8	19.5	3.7	3.1	—	—	—	—	—
H3k	970	35	51.4	10.8	12.6	9.0	6.4	—	—	—	—	—
H1 _{sol}	1085	45	12.2	9.0	4.4	5.6	2.4	—	—	—	—	—
H2 _{sol}	1210	32	3.8	2.3	19.5	3.8	3.2	—	—	—	—	—
H3 _{sol}	1035	60	139.9	43.8	4.4	21.0	20.8	—	—	—	—	—
H4 _{sol}	1100	30	10.9	7.4	19.5	4.8	4.2	—	—	—	—	—
H1 _{inj}	1450	15	0.3	0.1	144.3	0.4	0.06	1825	0.4	0.06	0.02	0.03
H2 _{inj}	1720	8	0.1	0.03	144.3	0.5	0.03	545	0.2	0.05	0.001	0.009
H3 _{inj}	1420	18	3.0	0.5	144.3	2.1	0.3	1965	1.6	0.3	0.01	0.06
H4 _{inj}	1525	10	0.2	0.03	216.8	0.6	0.07	865	0.5	0.1	0.009	0.01

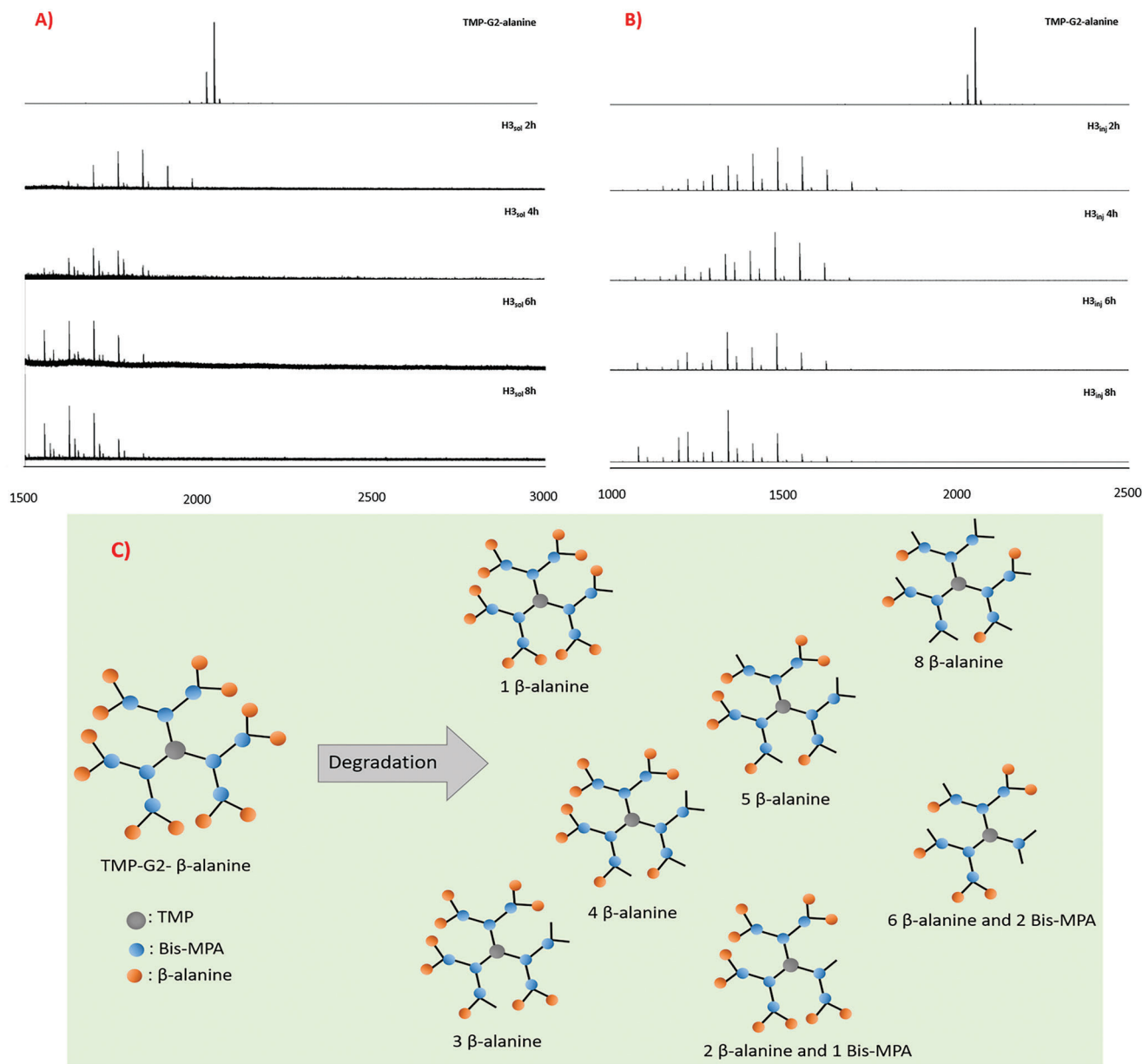


Figure 3. MALDI-TOF spectra of hybrid hydrogels. Representative spectra of leaching of TMP-G2-alanine from A) $H3_{sol}$ hydrogel and B) injectable hydrogel after 2, 4, 6, and 8 h in PBS at 37 °C, C) part of the degradation products based on the MALDI-TOF spectra.

A leaching-out study of the dendrimer and both the hybrid hydrogels were conducted in PBS solution (pH 7.4) at 37 °C. As shown in **Figure 3**, the MALDI-TOF spectrum of pure TMP-G2-alanine dendrimer with a single peak at 2058 m/z was compared with the spectra of the hybrid solid (**Figure 3A**) and injectable hydrogels (**Figure 3B**) at different time point. Multiple peaks at lower m/z were detected and that could be correlated to fragmented dendrimers that diffused out from the hydrogels. This suggests that the ionically integrated dendrimers undergo hydrolysis, through de-esterification of the peripheral beta-alanine groups, that in turn facilitate their detachment from the networks prior to release in PBS solution. Based on the analysis of MALDI peaks, the dendrimer lost its monodisperse integrity by fast los-

ing of the peripheral β -alanines.^[12] **Figure 3C** showed part of the representative degradation products, with the increase of time, Bis-MPA also de-attached from the dendrimers. Compared with $H3_{sol}$, degradation products from $H3_{inj}$ showed lower molecular weights and more loss of Bis-MPA, suggesting that the dendrimers are more stable and protected by $H3_{sol}$ hydrogels. No significant structural or leaching differences were detected in the spectra after 4 h for the $H3_{sol}$ hydrogel. A similar observation was found for $H3_{inj}$, which shows the presence of peaks correlated to dendrimer fragments after 4, 6, and 8 h. In contrast to the solid hybrid hydrogels, the dendrimers leached from the $H3_{inj}$ undergo accelerated degradation including the decomposition of the dendritic skeleton.

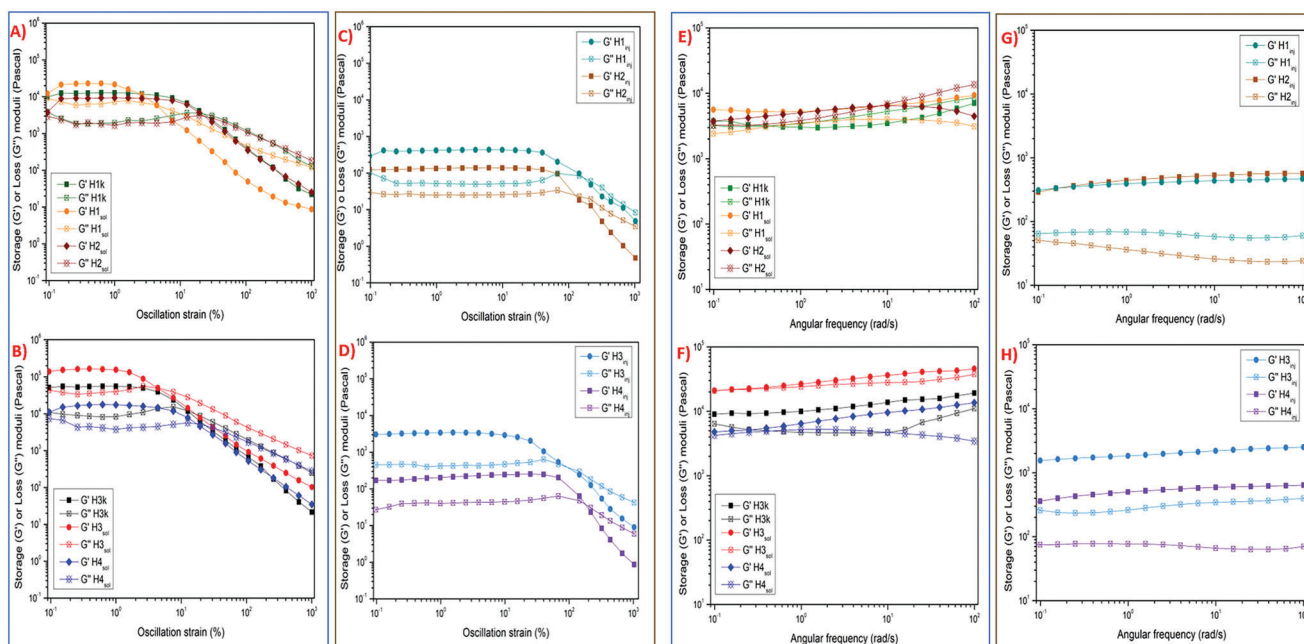


Figure 4. Amplitude sweep analysis of hybrid hydrogels. G' and G'' moduli of control, A,B) solid, and C,D) injectable hydrogels. Frequency sweep analysis of hybrid hydrogels. G' and G'' moduli of control, E,F) solid and G,H) injectable hydrogels.

These tunable hydrogels exhibited good viscoelastic strength and modulus comparable to human soft tissues.^[27] The rheological properties of all hybrid hydrogels were thoroughly investigated by frequency sweep analyses. **Figure 4E,F** shows the storage modulus (G') and the loss modulus (G'') of the solid hydrogels, while **Figure 4G,H** shows the moduli of the injectable hydrogels as a function of frequency. All hybrid and control hydrogels displayed G' higher than G'' in the studied frequency range, indicating that the hydrogels behaved as viscoelastic solids. The moduli of the solid hydrogels, H3_{sol} ($G' \approx 21.0$ kPa and $G'' \approx 20.8$ kPa) and H1_{sol} ($G' \approx 5.6$ kPa and $G'' \approx 2.4$ kPa) were noted higher than the control hydrogels, H3k ($G' \approx 9.0$ kPa and $G'' \approx 6.4$ kPa), and H1k ($G' \approx 3.7$ kPa and $G'' \approx 3.1$ kPa). Concerning the same mass ratio between GG-DA and TMP-G2-alanine, the solid hydrogels exhibited higher G' and G'' than their injectable counterpart. For example, H3_{sol} $G' \approx 21.0$ kPa and $G'' \approx 20.8$ kPa and H3_{inj} $G' \approx 2.1$ kPa and $G'' \approx 0.3$ kPa (all other data are included in Table 1).

The increased moduli are reflected by stronger intermolecular interactions in which the TMP-G2-alanine dendrimer enables the production of more tightly crosslinked 3D networks at the same concentration of GG-DA. It is also important to stark contrast in moduli between the hybrid hydrogels. In this case, an almost one order of magnitude in moduli difference between the solid hydrogel (H3_{sol} with $G' \approx 21.0$ kPa) and the injectable hydrogel (H3_{inj} with $G' \approx 0.5$ kPa). Regarding injectable hydrogels, the overall reduction in moduli is correlated to the crosslinking chemistry where quinone groups could form imine bonds, amine bonds, as well as physical interactions. The latter is an intriguing mode of crosslinking that provided the hydrogels with shear-thinning and self-healing behavior as shown in Videos S1–S3 (Supporting Information). When a self-healing hydrogel is applied to the wound site, it will be able to withstand the external force due to displacement.^[28] Preliminary amplitude sweep analyses of all hy-

brid hydrogels showed that initially, G' was higher than G'' . As shown in **Figure 4A–D**, at the LVE (Linear Viscoelastic Region), G' and G'' had a constant value, while a decrease was observed as the strain increased. A cross-point between G' and G'' was noted with increased strain, which indicates the critical point near which the hydrogel is in a state between solid and fluid. For the solid hydrogels, it is equal to a strain $< 10^2\%$, while for all injectable hydrogels, it is $> 10^2\%$. When the strain exceeded the critical strain point, G' dropped dramatically reaching values below G'' in which the hydrogel networks collapsed.^[29] Visual examination after the analysis revealed that the solid hydrogels were fragmented and broken while the injectable hydrogels were found intact and in a flow state. The latter is in fact due to the self-healing behavior as confirmed by the analysis of recovery times, **Figure 5C**.

Furthermore, the hydrogels possessed shear-thinning properties which is a critical property for use as injectable solutions for topical application, as shown in **Figure 5A** and Videos S1 and S2 (Supporting Information). To corroborate the results of the amplitude sweep analyses, recovery time measurements were further performed to test the rheology recovery behavior of the injectable hydrogels. The recovery and collapse behaviors of the hydrogels could be alternately looped, demonstrating a rapid and efficient self-healing ability. Indeed, after successive cycles of 100 s each, all injectable hydrogels recovered to their original values. The oscillatory shear strain was changed from 1% to 500% and was maintained for 100 s at each cycle. G' dropped from high values ≈ 230 –1678 Pa (H2_{inj}–H3_{inj}) to low values ≈ 2 –23 Pa (H2_{inj}–H3_{inj}) and subsequently recovered to their original high values. As seen in **Figure 5C**, the same self-healing behavior was observed for G'' , changing from high values ≈ 49 –309 Pa (H2_{inj}–H3_{inj}) to low values ≈ 8 –66 Pa (H2_{inj}–H3_{inj}). These results suggest that all injectable hydrogels, independent of moduli, show

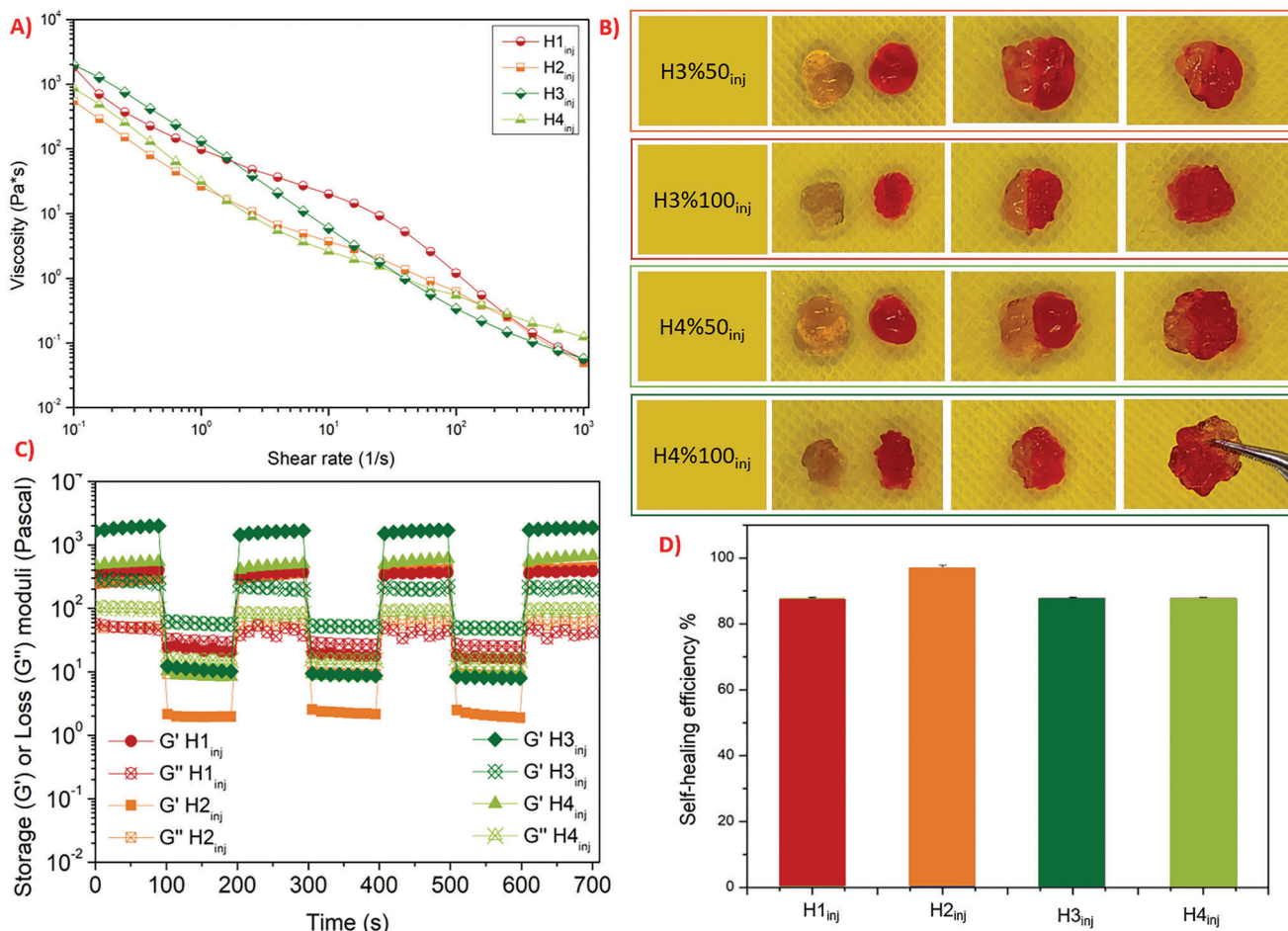


Figure 5. Shear-thinning and self-healing properties of the injectable hydrogels. A) Flow sweep analysis, B) macroscopic behavior of self-healing, C) recovery time analysis, and D) self-healing efficiency after seven cycles of recovery time analysis of injectable hybrid hydrogels.

rapid and almost full recovery after oscillatory shear deformation (Figure 5D). The self-healing behavior is also shown in Videos S3 and S4 (Supporting Information), where it is noted that two pieces of the same hydrogel (one colored with Rhodamine B and one uncolored) if placed in contact unite and reform as a single piece.

Obtaining a biomaterial with intrinsic tissue adhesive properties is advantageous as it would ensure permanence on the wound bed without it being washed away by biological fluids, thus ensuring minimal damage to the wound and a real improvement in patient compliance.^[30] Hydrogel H1_k, H1_{sol}, and H1_{inj} exemplify the adhesion to a wide variety of substrates **Figure 6**. All hybrid hydrogels produced showed a similar ability to adhere to glass, plastic, metal, aluminum foil, wood, and raw pig skin. The adhesive property of the hydrogels is probably due to the presence of cationic amino groups as well as catechol groups, as confirmed by the adhesion of the control hydrogels.^[31] Notably, the hybrid hydrogels also resist strong shocks and bending as demonstrated in Videos S5 and S6 (Supporting Information). This confirms the uniqueness of the hybrids hydrogels as adhesive networks with potential use as coatings or implantable materials that could be applied directly into the wound without the need for additional fixation or other supports.

2.3. Cytocompatibility of the Hybrid Hydrogels

Producing a suitable microenvironment in the form of cytocompatible hydrogels where cells can survive and grow for wound healing is one of the most important factors. Consequently, a study was performed on three different cell lines: Fibroblasts (HDFs), Keratinocytes (HaCaT), and macrophages (RAW 264.7). These cells are known to play important roles in normal skin wound healing and several studies detail their involvement in cellular therapy processes. HDFs are cells that directly deposit extracellular matrix proteins during the healing process,^[32,33] while HaCaT have the ability to form a large sheet of epidermis that improves wound closure and epithelialization.^[32,34] Inflammatory signals trigger the proliferation and maturation of these two cell types, which are essential for wound healing.^[35] Macrophages and monocytes (RAW 264.7) improve the healing rate of wounds.^[36] A cytocompatibility test was performed by applying all hydrogels in direct contact with the three aforementioned cell lines, **Figure 7**. For the control hydrogels without the presence of dendrimers, H1_k and H3_k, the cytocompatibility was found good. In the case of the hybrid networks, the solid hydrogels indicated good cytocompatibility in which H4_{sol} and H2_{sol} with a lower concentration of dendrimers showed overall

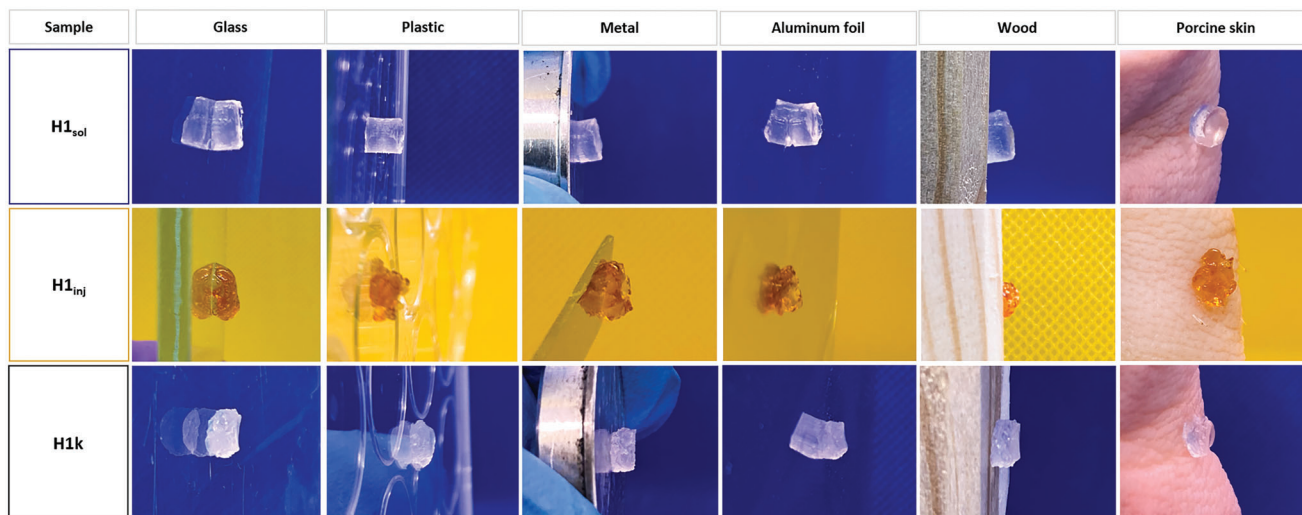


Figure 6. The adhesiveness of the hybrid and control hydrogels on different substrates.

higher cell viability compared to hydrogels with a higher concentration of dendrimers, H3_{sol} and H1_{sol}. Similarly, for the injectable hydrogels, H4_{inj} and H2_{inj} exhibited overall higher cell viability than the hydrogels with increased concentration of dendrimers, H3_{inj} and H1_{inj}. It should also be noted that the injectable hydrogels have slightly better cytocompatibility profiles

than their solid counterpart. This is probably a production-related effect as the solid hydrogels required a pH increase of the precursor GG-DA > 8.5, to oxidize the catechol groups, before adding the TMP-G2-alanine. The presence of quinone in the hybrid hydrogels could promote the cells to withstand oxidative stress and thereof affect cell growth.^[28] For both solid and injectable

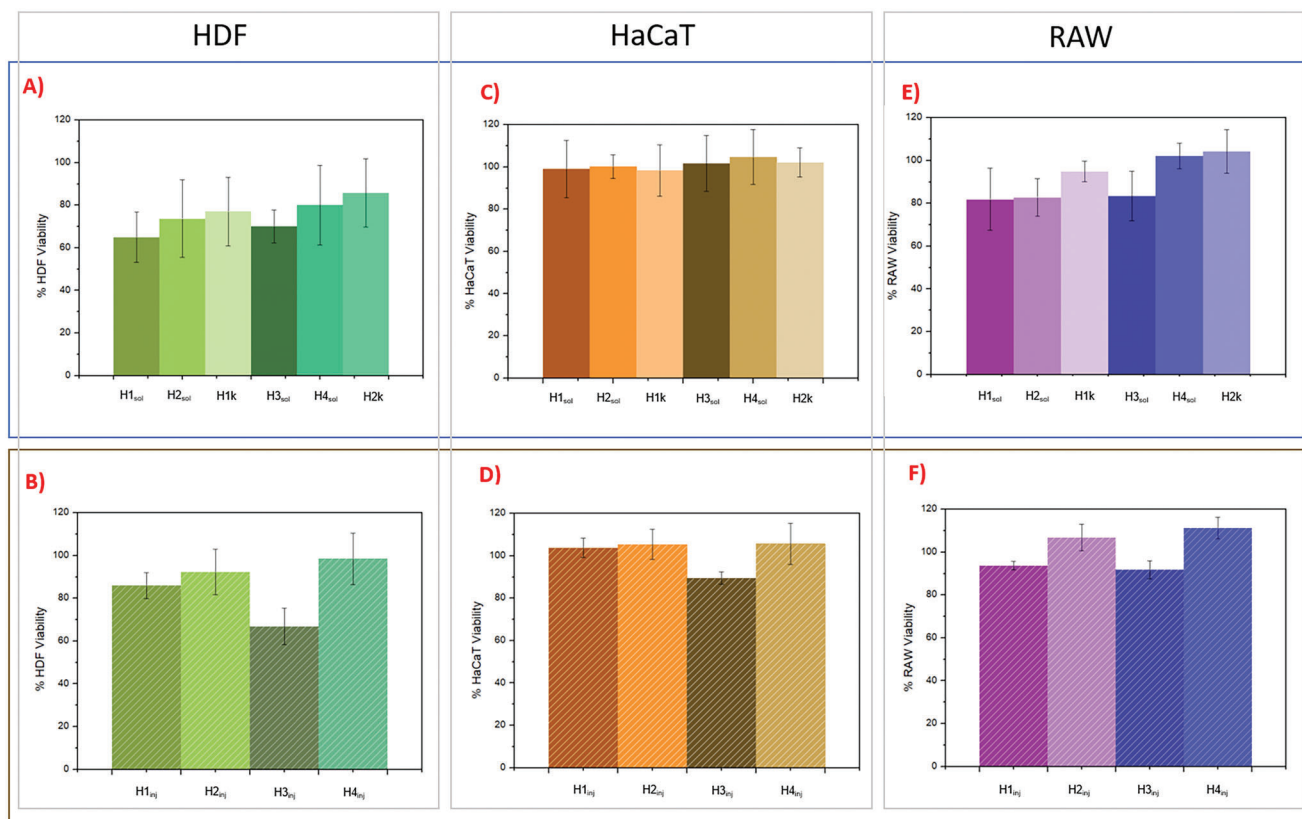


Figure 7. The cytocompatibility of the A) solid and B) injectable hybrid hydrogels tested with HDF cells; C) solid and D) injectable hybrid hydrogels tested with HaCaT cells, and E) solid and F) injectable hybrid hydrogels tested with RAW cells. All data are shown as a mean value ± SD ($n = 3$).

Table 2. MIC and MBC Values of TMP-G2-alanine and GG-DA.

Measurement	Sample	<i>E.coli</i> 178			<i>S.aureus</i> 2569		
		$\mu\text{g mL}^{-1}$	μM	NH_3^+ [μM]	$\mu\text{g mL}^{-1}$	μM	NH_3^+ [μM]
MIC value	TMP-G2-alanine	62,5	18,4	221	250	73,6	882
	GG-DA	>2000			>2000		
MBC value	TMP-G2-alanine	125	36,8	441	500	147,1	1765
	GG-DA	>2000			>2000		

hydrogels, incubation with RAW and HaCaT cells showed better viability than HDF. For example, cell viability of H4_{sol} in HDFs was 80%, HaCaTs of 105%, and RAW 264.7 of 102%; while with H4_{inj} the HDF had a viability of 98%, the HaCaT of 106% and the RAW of 111%. These findings indicate that both solid and injectable H4 hydrogels are safe to use as they enhance cell proliferation of both RAW 264.7 cells and HaCaT cells and maintained good HDF viability. Neither solid nor injectable hydrogels possess cytotoxic effects toward HaCaTs, with viability around or >100% in all cases, which formed a monolayer of cells after 24 h co-incubation with hydrogels. Collectively, these hybrid hydrogels show great promise as skin wound dressings in which the cells maintain normal cell morphology, comparable to the cell-alone control, Figures S9–S11 (Supporting Information).

2.4. Antimicrobial Studies of the Hybrid Hydrogels

The antibacterial property of the cationic dendrimer, TMP-G2-alanine, was investigated using MIC and MBC assays. Two types of bacteria were used in the study, *S. aureus* 2569 (Gram-positive) and *E. coli* 178 (Gram-negative).^[37] The MIC and MBC values for the cationic dendrimer showed good antibacterial properties against both bacteria, **Table 2**. The results also detailed that higher dendrimer concentrations were required to kill *S. aureus* than *E. coli*, suggesting greater efficiency against Gram- than Gram+ strains. The MIC and MBC values of GG-DA are above 2 mg mL^{-1} , indicating that the pure polymer has no obvious antibacterial properties.

All hybrid solid hydrogels exhibited antibacterial properties with inhibition zones visible on the agar plate against both *E.*

coli 178 and *S. aureus* 2569, as shown in Figure S12 (Supporting Information). The antimicrobial test in bacterial solution (10^5 CFU mL^{-1}) with the two bacterial strains demonstrated that both solid and injectable hydrogels possess good activity against both *S. aureus* and *E. coli*, **Figure 8**. In particular, solid hydrogels possessed a great sterilizing mode-of-action with 100% killing for both *S. aureus* and *E. coli* already after 4 h incubation. On the other hand, the injectable hydrogels showed a decreasing antibacterial activity over time. A plausible explanation is related to the dendrimers that are covalently bound within the networks which inhibit their leaching out compared with the solid hydrogels. This was confirmed by the inhibition zones and increased degradation of the dendrimer as corroborated by the leaching analyses, Figure 3. Similar to the dendrimer, the hydrogels with increased dendrimer concentration resulted in higher antibacterial activity. Hydrogels with higher concentrations of initial dendrimer showed higher killing efficiency of bacteria after 4 h. H1_{inj} showed 100% of the killing of *E. coli* and H3_{inj} of 98%; while H1_{inj} killed 90% and H3_{inj} 94% of *S. aureus*. The hydrogels with lower initial concentrations of dendrimer instead showed a lower killing efficiency of both bacterial strains after 4 h. H2_{inj} showed a killing % of *E. coli* of 93% and H4_{inj} of 96%; while H2_{inj} killed 82% and H2_{inj} 81% of *S. aureus*.

3. Conclusion

In conclusion, two new types of biocompatible and degradable polysaccharide/dendritic hybrid hydrogels have been developed by exploiting in the first case the electrostatic interactions occurring between the two biomaterials and subsequently exploiting

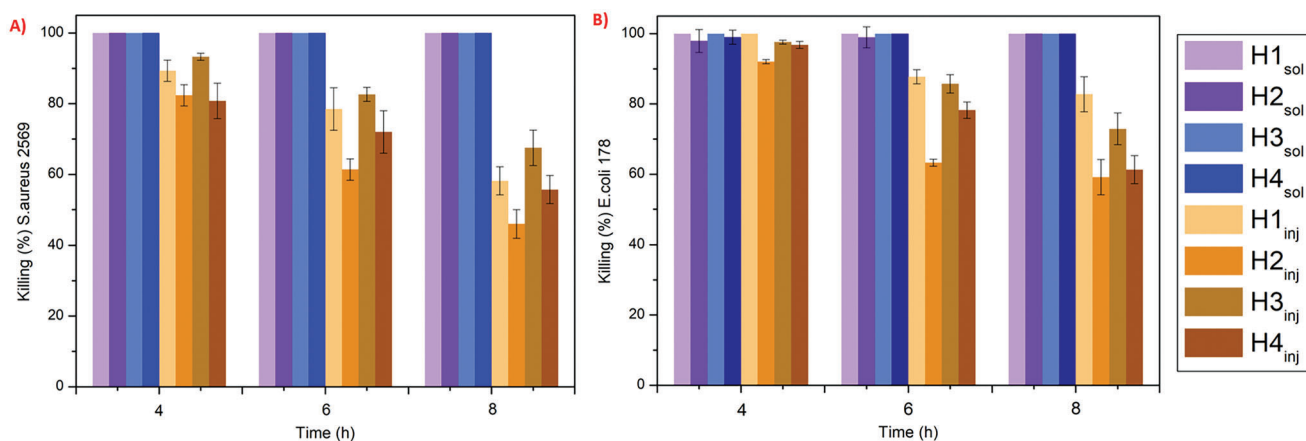


Figure 8. Antimicrobial activity of hybrid hydrogels against A) *S. aureus* 2569 and B) *E. coli* 178. All data are shown as a mean value \pm SD ($n = 3$).

an ionotropic crosslinking with Ca²⁺ ions and in another case the formation of dynamic imine bonds between the dopamine on the polysaccharide backbone and the amino groups of the dendrimer. Hybrid hydrogels possess flexible and tunable viscoelastic properties with storage modulus in the range of ≈21.0–3.2 kPa for solid hydrogels, and in the range of ≈2.1–0.5 kPa for injectable ones. The injectable hybrid hydrogels also exhibited shear-thinning and self-healing behavior, meeting flexural and motion requirements when injected into soft tissue. Furthermore, after in vitro co-culture, most hydrogels showed good biocompatibility toward HDF, HaCaT, and RAW, indicating their great potential as dressing materials. Antimicrobial testing with two common bacterial strains characteristic of Gram⁺ and Gram⁻, *S. aureus* and *E. coli*, demonstrated that solid hydrogels cause complete eradication of bacteria after a few hours and injectable hydrogels cause a significant bacteria decrease. The results suggest that by using these two precursor materials it is possible to obtain adjustable systems for multiple applications. The two types of biocompatible and degradable hybrid hydrogels are in fact promising antibacterial systems that could be applied as dressings to prevent or treat bacterial infections.

4. Experimental Section

Chemicals: Low molecular weight GG was produced as previously reported.^[20] Starting GG (Gelzan CM), tetrabutylammonium hydroxide (TBA-OH), bis (4-nitrophenyl) carbonate (4-NPBC), dopamine hydrochloride (DA), sodium chloride (NaCl), acetone, anhydrous dimethyl sulfoxide (DMSO), Dowex 50WX8 resin, sodium hydroxide (NaOH), calcium chloride (CaCl₂), phosphate buffer (Dulbecco's Phosphate-Buffered Saline DPBS), and deuterium oxide (D₂O) were purchased from Merck (Italy). TMP-G2-alanine synthesized as previously reported.^[12] Dulbecco's modified Eagle medium (DMEM) fetal bovine serum (FBS), penicillin-streptomycin, glutamine, and amphotericin B, Calcein AM and Alamar Blu reagent were purchased from Thermo Fisher Scientific. Mueller–Hinton broth (MHB II) was purchased from Fluka. MHB II agar was from Sigma-Aldrich.

Bacteria Strains and Cells Lines: *Escherichia coli* 178 (*E. coli* 178) was kindly provided by Prof. Paul Orndorff from North Carolina State University. *Staphylococcus aureus* 2569 (*S. aureus* 2569) was obtained from the company DSMZ. Human dermal fibroblast (HDF) and mouse monocyte (RAW 264.7) cells were purchased from the American Tissue Culture Collection (ATCC). Human epidermal keratinocyte (HaCaT) cells were obtained from kindly provided by Prof. Annelie Brauner from Karolinska Institutet.

Instruments: Fourier-transform infrared spectroscopy (FT-IR) was performed with a Perkin–Elmer spotlight 400 FTIR system (Waltham, MA, USA) equipped with a single reflection attenuated total reflectance (ATR) in the region of 600–4000 cm⁻¹. The rheological tests were carried out using a DHR-2 TA Instrument oscillatory rheometer equipped with a flat geometry of 8 mm in diameter (TA Instruments – Waters S.p.A.). The optical microscope images were acquired through the Eclipse Ti microscope (Nikon). Scanning electron microscopy (SEM) analyses were conducted using S-4800 field emission scanning electron microscope (Hitachi, Tokyo, Japan).

Hydrogel Production: The hydrogels were produced by dispersing GG-DA, synthesized as described in Supporting Information, in DI water (80 °C 10 min). The TMP-G2-alanine, synthesized as previously reported,^[12] was dispersed in DI water at the w/w concentration with respect to the GG-DA shown in Table 3. For the formation of hydrogels, two different approaches were used. four solid and four injectable hydrogels were produced. The pH was adjusted to 6.5 before mixing the two solutions to produce the hybrid solid hydrogels. Briefly, these solids hydrogels

Table 3. Composition of hybrid hydrogels.

Hydrogels (total volume: 1 ml)	Amount GG-DA	Amount TMP-G2-alanine
	mg	mg
H1 _{sol or inj}	30	30
H2 _{sol or inj}	30	15
H3 _{sol or inj}	40	40
H4 _{sol or inj}	40	20
H1k	30	–
H3k	40	–

were produced by dispersing dendrimer and polymer at the concentrations shown in Table 3. The two solutions were injected and vortexed for 1 min, then these hydrogels were placed in 0.1 M CaCl₂ (1 ml) for 1 h to 4 °C and then washed twice with DI water. As controls, two hydrogels were produced using only the solution of GG-DA at 3% and 4% w/v and placing them in 0.1 M CaCl₂ for 1 h at 4 °C and then washed twice with DI water. The pH of GG-DA was also adjusted to 8.5 with 0.1 M NaOH, until the solution became brown, to produce the hybrid injectable hydrogels. In particular, the injectable hydrogels were prepared gently mixing directly both the solutions of GG-DA and TMP-G2-alanine into the vial, until the solution became homogeneous. Then the hydrogel was placed in a syringe using the pipette for viscous solutions HandyStep.

Characterizations: FT-IR, SEM, swelling test, in vitro degradability of the hydrogels, viscoelastic profiles of hydrogels over time of degradation, and macroscopic adhesiveness properties were performed to study the physical and chemical properties of the hydrogels. The details are available in the Supporting Information.

Leaching Analysis of the Hybrid Hydrogels: A leaching study of both hybrid solid and injectable hydrogels was conducted in DPBS solution (pH 7.4) at 37 °C. The hybrid hydrogels (formed with a total volume of 50 μL) were prepared and immersed in DPBS (1 ml), 5 μL aliquots were collected at different time intervals of 1, 2, 4, and 8 h, and the components of the samples were further analyzed by MALDI-TOF-MS.

Rheological Characterization: For rheological experiments, all of the hydrogels (50 μL) were placed on a parallel plate geometry with an 8 mm diameter upper plate. The LVE (Linear Viscoelastic region) was preliminarily assessed by strain sweep experiments applying a constant frequency of 1 Hz and an oscillation strain % between 0.01% and 1000% at 25 °C. The measurement gap was set at 500 μm for all analyses. Viscoelastic properties were evaluated also at 25 °C by performing frequency sweep measurements in the range 0.01–100 Hz by applying a constant strain% of 0.1%. For the injectable hydrogels were also studied the shear-thinning and the self-healing behaviors. The shear-thinning properties were studied through the flow-sweep study for shear rates between 0.1 and 1000 (1/s). The self-healing capacity was evaluated through the recovery time study. The samples were subjected to seven cycles, each lasting 100 s, alternating a low strain% (1%) to a high strain% (500%), applying a frequency of 0.1 Hz. All experiments were performed in triplicate at a temperature of 25 °C.

The self-healing of the samples was calculated as:

$$\text{Self-healing efficiency \%} = \frac{G'_2}{G'_1} \times 100 \quad (1)$$

Where G'_1 is the original storage modulus of the sample and G'_2 is its storage modulus after large strain failure, according to the rheological data.

Each experiment was performed in triplicate and results were expressed as mean value ± standard deviation.

Cytotoxicity Tests: Fifty microliters of each of the cylinder-shaped hydrogels were previously sterilized by UV lamp and they were placed directly into a 48-well plate containing 1×10^4 cells (HDF, HaCaT, and RAW)

seeded 24 h earlier with another fresh medium (total amount 1 ml). After 24 h, Alamar Blue was added and the incubation was continued for 4 h (37 °C, 5% CO₂). The fluorescence intensity was measured at ex/em 560/590 nm for the Alamar Blue assay. The images, shown in the Supporting information, were acquired with the Eclipse Ti microscope (Nikon). All experiments were conducted in triplicate.

Antibacterial Assays of the Hybrid Hydrogels: The antibacterial property of the hybrid hydrogels was tested using the disc diffusion test using *E. coli* 178 and *S. aureus* 2569, as described in the Supporting information.

The antibacterial property of the 50 µl cylindrical hybrid hydrogels was also tested in bacterial solution. *E. coli* 178 and *S. aureus* 2569 were cultured in MHB II broth at 37 °C with shaking of 250 rpm overnight. Each bacterial solution at the log phase was diluted to a concentration of 10⁵ CFU/mL. Then the cylindrical hybrid hydrogels were added into a 48-well plate, where each well contained 1 ml of bacterial solution, and the plate was transferred into the incubator and incubated at 37 °C for 4, 6, and 8 h. After the incubation, the plate counting method was used to calculate the bacterial concentrations in the wells. Wells without the treatment of hydrogels were used as a positive control. All measurements were performed in triplicate.

Supporting Information

Supporting Information is available from the Wiley Online Library or from the author.

Conflict of Interest

The authors declare no conflict of interest.

Data Availability Statement

The data that support the findings of this study are available from the corresponding author upon reasonable request.

Keywords

adhesive catechol-gellan gum, antimicrobial, dendritic hybrid hydrogels, dopamine, gellan gum, self-healing hydrogel, wound healing

Received: May 18, 2023

Revised: July 31, 2023

Published online:

- [1] V. W. L. Ng, J. M. W. Chan, H. Sardon, R. J. Ono, J. M. García, Y. i. Y. Yang, J. L. Hedrick, *Adv. Drug Deliv. Rev.* **2014**, *78*, 46.
- [2] S. Wang, H. Zheng, L. i. Zhou, F. Cheng, Z. Liu, H. Zhang, L. Wang, Q. Zhang, *Nano Lett.* **2020**, *20*, 5149.
- [3] Y. Dong, Y. Zheng, K. Zhang, Y. Yao, L. Wang, X. Li, J. Yu, B. Ding, *Adv. Fiber Mater.* **2020**, *2*, 212.
- [4] S. Macneil, *Nature* **2007**, *445*, 874.
- [5] X. Zhao, H. Wu, B. Guo, R. Dong, Y. Qiu, P. X. Ma, *Biomaterials* **2017**, *122*, 34.
- [6] W.-C. Huang, R. Ying, W. Wang, Y. Guo, Y. He, X. Mo, C. Xue, X. Mao, *Adv. Funct. Mater.* **2020**, *30*, 2000644.
- [7] N. Sood, A. Bhardwaj, S. Mehta, A. Mehta, *Drug Delivery* **2014**, *23*, 748.
- [8] N. M. Milovic, J. Wang, K. Lewis, A. M. Klibanov, *Biotechnol. Bioeng.* **2005**, *90*, 715.
- [9] A. Jain, L. S. Duvvuri, S. Farah, N. Beyth, A. J. Domb, W. Khan, A. Jain, L. S. Duvvuri, W. Khan, S. Farah, A. J. Domb, N. Beyth, *Adv. Healthcare Mater.* **2014**, *3*, 1969.
- [10] M. K. Calabretta, A. Kumar, A. M. Mcdermott, C. Cai, *Biomacromolecules* **2007**, *8*, 1807.
- [11] A. Labena, K. I. Kabel, R. K. Farag, *Mater. Sci. Eng., C* **2016**, *58*, 1150.
- [12] P. Stenström, E. Hjorth, Y. Zhang, O. C. J. Andrén, S. Guette-Marquet, M. Schultzberg, M. Malkoch, *Biomacromolecules* **2017**, *18*, 4323.
- [13] O. C. J. Andrén, T. Ingverud, D. Hult, J. Håkansson, Y. Bogestål, J. S. Caous, K. Blom, Y. Zhang, T. Andersson, E. Pedersen, C. Björn, P. Löwenhielm, M. Malkoch, *Adv. Healthcare Mater.* **2019**, *8*, 1801619.
- [14] A. W. Bosman, H. M. Janssen, E. W. Meijer, *Chem. Rev.* **1999**, *99*, 1665.
- [15] M. Ghirardello, K. Öberg, S. Staderini, O. Renaudet, N. Berthet, P. Dumy, Y. Hed, A. Marra, M. Malkoch, A. Dondoni, *J. Polym. Sci. A Polym. Chem.* **2014**, *52*, 2422.
- [16] P. Wu, M. Malkoch, J. N. Hunt, R. Vestberg, E. Kaltgrad, M. G. Finn, V. V. Fokin, K. B. Sharpless, C. J. Hawker, *Chem. Commun.* **2005**, 5775.
- [17] Y. Fan, F. Namata, J. Erlandsson, Y. Zhang, L. Wågberg, M. Malkoch, *Pharmaceutics* **2020**, *12*, 1139.
- [18] F. S. Palumbo, S. Federico, G. Pitarresi, C. Fiorica, G. Giammona, *Carbohydr. Polym.* **2020**, *229*, 115430.
- [19] C. Fiorica, F. S. Palumbo, G. Pitarresi, G. Biscari, A. Martorana, C. Calà, C. M. Maida, G. Giammona, *Int. J. Pharm.* **2021**, *610*, 121231.
- [20] C. Fiorica, G. Biscari, F. S. Palumbo, G. Pitarresi, A. Martorana, G. Giammona, *Gels* **2021**, *7*, 62.
- [21] Y. Liang, J. He, B. Guo, *ACS Nano* **2021**, *15*, 12687.
- [22] A. Zhang, Y. a. Liu, D. i. Qin, M. Sun, T. Wang, X. Chen, *Int. J. Biol. Macromol.* **2020**, *164*, 2108.
- [23] C. Watters, T. T. Yuan, K. P. Rumbaugh, *Chronic Wound Care Manag. Res.* **2015**, *2*, 53.
- [24] J. Yang, M. A. Cohen Stuart, M. Kamperman, *Chem. Soc. Rev.* **2014**, *43*, 8271.
- [25] M. Naseri-Nosar, Z. M. Ziora, *Carbohydr. Polym.* **2018**, *189*, 379.
- [26] Y. e. Ma, L. Xin, H. Tan, M. Fan, J. Li, Y. Jia, Z. Ling, Y. Chen, X. Hu, *Mater. Sci. Eng., C* **2017**, *81*, 522.
- [27] X. Chen, *Small Methods* **2017**, *1*, 1600029.
- [28] X. Zhao, Y. Liang, Y. Huang, J. He, Y. Han, B. Guo, *Adv. Funct. Mater.* **2020**, *30*, 1910748.
- [29] Z. Wei, J. H. Yang, Z. Q. i. Liu, F. Xu, J. X. Zhou, M. Zrínyi, Y. Osada, Y. M. Chen, *Adv. Funct. Mater.* **2015**, *25*, 1352.
- [30] M. Waring, S. Bielfeldt, M. Brandt, **2009**.
- [31] L. Fischer, A. K. Strzelczyk, N. Wedler, C. Kropf, S. Schmidt, L. Hartmann, *Chem. Sci.* **2020**, *11*, 9919.
- [32] H. i.-J. You, S.-K. Han, *J. Korean Med. Sci.* **2014**, *29*, 311.
- [33] M. Edmonds, E. and A.A.D.F.U.S. Group, *Int. J. Low Extrem. Wounds* **2009**, *8*, 11.
- [34] L. P. Da Silva, R. L. Reis, V. M. Corrello, A. P. Marques, *Annu. Rev. Biomed. Eng.* **2019**, *21*, 145.
- [35] A. M. Wojtowicz, S. Oliveira, M. W. Carlson, A. Zawadzka, C. F. Rousseau, D. Baksh, *Wound Repair Regener.* **2014**, *22*, 246.
- [36] M. S. Hu, G. G. Walmsley, L. A. Barnes, K. Weiskopf, R. C. Rennert, D. Duscher, M. Januszzyk, Z. N. Maan, W. X. Hong, A. T. M. Cheung, T. Leavitt, C. D. Marshall, R. C. Ransom, S. Malhotra, A. L. Moore, J. Rajadas, H. P. Lorenz, I. L. Weissman, G. C. Gurtner, M. T. Longaker, *JCI Insight* **2017**, *2*, e96260.
- [37] G. Pitarresi, G. Barberi, F. S. Palumbo, D. Schillaci, C. Fiorica, V. Catania, S. Indelicato, D. Bongiorno, G. Biscari, G. Giammona, *Int. J. Mol. Sci.* **2022**, *23*, 15378.